doi:10.1016/j.jmb.2006.03.066 J. Mol. Biol. (2006) 359, 509–525

JMB

Available online at www.sciencedirect.com

SCIENCE DIRECT®

ELSEVIER

REVIEW

Structural Basis for Diversity of the EF-hand Calcium-binding Proteins

Zenon Grabarek

Boston Biomedical Research Institute, Watertown, MA 02472, USA

The calcium binding proteins of the EF-hand super-family are involved in the regulation of all aspects of cell function. These proteins exhibit a great diversity of composition, structure, Ca^{2+}-binding and target interaction properties. Here, our current understanding of the Ca^{2+}-binding mechanism is assessed. The structures of the EF-hand motifs containing 11–14 amino acid residues in the Ca^{2+}-binding loop are analyzed within the framework of the recently proposed two-step Ca^{2+}-binding mechanism. A hypothesis is put forward that in all EF-hand proteins the Ca^{2+}-binding and the resultant conformational responses are governed by the central structure connecting the Ca^{2+}-binding loops in the two-EF-hand domain. This structure, named EFβ-scaffold, defines the position of the bound Ca^{2+}, and coordinates the function of the N-terminal (variable and flexible) with the C-terminal (invariable and rigid) parts of the Ca^{2+}-binding loop. It is proposed that the nature of the first ligand of the Ca^{2+}-binding loop is an important determinant of the conformational change. Additional factors, including the interhelical contacts, the length, structure and flexibility of the linker connecting the EF-hand motifs, and the overall energy balance provide the fine-tuning of the Ca^{2+}-induced conformational change in the EF-hand proteins.

© 2006 Elsevier Ltd. All rights reserved.

Keywords: EF-hand; calcium binding proteins; structure and function; calcium signaling

Introduction

The term "EF-hand" was coined by R. H. Kretsinger over 30 years ago for the Ca^{2+}-binding variant of a helix-loop-helix motif discovered in the structure of parvalbumin, a small Ca^{2+}-binding protein isolated from carp muscle.[1] The EF-hand motifs were then identified in the amino acid sequence of troponin C,[2] the myosin light chains,[3] the ubiquitous calmodulin,[4,5] and in many other Ca^{2+}-binding proteins.[6,7] Today, there are more than 3000 EF-hand related entries in the NCBI Reference Sequences Data Bank. Calcium and the EF-hand Ca^{2+}-binding proteins have been recognized as the key players in all aspects of cell function, starting with a cell's birth during mitosis and ending with its apoptotic death.[8–11] At the most fundamental level, these diverse cellular functions are triggered by the simple event of the Ca^{2+} attracting six to seven oxygen atoms of the EF-hand. The EF-hand proteins' role is to "translate" that simple regulatory signal into various functional responses. The exceptional versatility of the EF-hand motif is clearly reflected in the growing database of three-dimensional structures of EF-hand proteins revealing a great diversity of conformations, domain organization, and structural responses to calcium.[12,13] However, our understanding of the structural principles that underlie this versatility and govern the function of EF-hand proteins is far from adequate. The problem is that there are still very few proteins for which the high-resolution X-ray crystallographic structures of both the apo and the Ca^{2+}-bound forms are available. In recent years remarkable progress has been made owing to the development and use of NMR techniques, which provide invaluable information on the dynamical properties of the EF-hand proteins and enable study of transient conformational states.[14–18] Unfortunately, NMR techniques do not provide sufficiently precise

Abbreviations used: CaM, calmodulin; TnC, troponin C; PDB, Protein Data Bank.

E-mail address of the author grabarek@bbri.org

0022-2836/$ - see front matter © 2006 Elsevier Ltd. All rights reserved.

information on the calcium-binding loops,[19] which are of particular interest since the calcium ligands are critical for transmitting the conformational changes associated with the Ca^{2+}-binding event to the rest of the protein.

There are several excellent reviews on the structure and function of calcium-binding proteins. An extensive analysis of the Ca^{2+}-binding sites in proteins can be found in the article by McPhalen *et al.*[20] The EF-hand proteins specifically are discussed by Strynadka & James.[21] The diversity in the organization, packing and response to Ca^{2+} in EF-hand proteins was reviewed by Nelson & Chazin.[12] and most recently by Ikura & Ames.[22] Evenas *et al.*[23] published an overview of the intra- and extra-cellular Ca^{2+}-signaling from the structural perspective. There are several reviews focused on the Ca^{2+}-binding properties of the EF-hand proteins,[24–28] and on the target binding mechanisms.[29–35] A selection of articles covering broad aspects of Ca^{2+}-signaling can be found in the book edited by Ernesto Carafoli & Claude Klee.[36] Finally, specific information on each of the many subfamilies of EF-hand proteins can be found in dedicated reviews, too numerous to list here.

The present work is focused on the mechanism by which Ca^{2+} drives the conformational change in EF-hand proteins. Selected high-resolution X-ray crystallographic structures of EF-hand proteins representative of diverse families are analyzed within the framework of the recently proposed two-step Ca^{2+}-binding mechanism[37] and compared in a conformation-independent frame of reference. A hypothesis is put forward that Ca^{2+}-binding and the resultant conformational response in all two-EF-hand domains is governed by the central structure named EFβ-scaffold. Some structural features of the EF-hand motif that shape the conformational change are discussed.

Structure of the EF-hand

The most common (canonical) EF-hand has a 12-residue Ca^{2+}-binding loop that starts with an aspartate and ends with a glutamate. The Ca^{2+}–ligand geometry in small molecule-Ca^{2+} complexes is octahedral, which when applied to the Ca^{2+}–EF-hand complex provides a convenient assignment of the ligands in the orthogonal coordinate system centered on the Ca^{2+}, and the *X*,*Y*,*Z* axes defined by the first three Ca^{2+} ligands of the loop. However, in most EF-hand proteins Ca^{2+} is linked to seven oxygen atoms arranged in a pentagonal bipyramid. The Glu residue in the last position of the loop ($-Z$ ligand) contributes two oxygen atoms of its γ-carboxyl group (a bidentate ligand). In all known structures of EF-hand proteins the central residue of the Ca^{2+}-binding loop (the $-Y$ position) binds Ca^{2+} with the main-chain carbonyl oxygen atom. Next to this residue, there is a hydrophobic amino acid (most frequently Ile, Val or Leu) that makes two hydrogen bonds to the equivalent residue of the paired EF-hand, a part of the short β-sheet connecting the two Ca^{2+}-binding loops [21].

The composition and the length of the Ca^{2+}-binding loops vary significantly among the EF-hand proteins. The N-terminal EF-hand in calbindin D9k, the vitamin D-dependent calcium binding protein from intestine, has a 14-residue loop and except for the C-terminal glutamate, all protein ligands are the main-chain carbonyl oxygen atoms.[38,39] Despite such radical departure from the "normal" mode of binding, the pentagonal bipyramid Ca^{2+}-ligand geometry and the high affinity for Ca^{2+} are preserved. This variant of the EF-hand motif referred to as the pseudo EF-hand is found in members of the S100 protein family. More recently, structures of EF-hand proteins containing an 11-residue Ca^{2+}-binding loop (calpain,[40,41] grancalcin,[42] ALG-2[43]) or a 13-residue loop (SPARC/osteonectin/BM-40[44]) became available and provided evidence that similar pentagonal bipyramid geometry of Ca^{2+}-coordination can be achieved in several different ways. In Table 1 there are examples of amino acid sequences of various EF-hand motifs. It is striking that all the insertions and deletions are localized in the N-terminal part of the loop, whereas the C-terminal part is constant in length. Differences in the loop length and composition lead to different backbone folding, and often the main-chain carbonyl oxygen atoms are involved in Ca^{2+}-binding. It appears that the Ca^{2+}-binding ligand is defined by the backbone conformation. For example in calcyclin (the S100A6 protein) Glu23 (*Y* position) and Asp25 (*Z* position) bind Ca^{2+} with their main-chain carbonyl rather than the side-chain carboxyl groups. Yet, some structural flexibility is possible. Cates *et al.*[45] found that a substitution of Ala for Asp in the first position of the Ca^{2+}-binding loop II of parvalbumin causes the incoming helix to shift slightly to enable the main-chain carbonyl oxygen to substitute for the missing carboxyl. The variability of the N-terminal part of the Ca^{2+}-binding loop is, in fact, much greater than the examples in Table 1 might suggest. The EF-hand I of CIB1, a protein related to the neuronal calcium sensors (NCS) has a 20-residue loop[46] (PDB code 1XO5) and KChIP1, the Kv4 K^+ channel interacting protein has an EF-hand with a ten-residue loop[47] (PDB code 1S1E). Neither loop is capable of Ca^{2+}-binding, but the respective domains preserve the general EF-hand topology including the short β-sheet hydrogen bonding with the pair-mate EF-hand.

The glutamate residue in the last coordinating position and its fixed spacing from the $-Y$ ligand appear to be required for the pentagonal bipyramid coordination geometry. Departure from this rule leads to a different Ca^{2+}-ligand geometry. One example is the substitution of Asp for Glu in the $-Z$ position of EF-hand I in the regulatory light chain of myosin (Table 1), which leads to preference for Mg^{2+} and octahedral Ca^{2+} coordination.[48] In the essential light chain of scallop myosin a substitution of Lys for the C-terminal Glu is compensated by an

Table 1. Variability in the amino acid sequence of the EF-hand Ca^{2+}-binding motif

loop length	protein	starting residue	amino acid sequence										
			incoming helix								*exiting helix*		*linker*
				Ca^{2+}-*binding loop*									
				X		**Y**	**Z**		**-Y**	-X	**-Z**		
14	calcyclin	4	PLDQAIGLLVAIFHKY	**S**	G	R	**E**	G	**D**	K	H	**T**	**L**	SKK**E**	LKELIQKE	LTIGSKLQ
14	calbindin D9k	3	PEELKGIFEKY	**A**	A	K	**E**	G	**D**	P	N	**Q**	**L**	SKE**E**	LKLLLQTE	FPSLLKGPST
13	osteonectin	207	YNMYIFPVHWQFGQL	**D**	Q	H	**P**	I	**D**	-	G	**Y**	**L**	SHT**E**	LAPLR	APLIPM
12	calmodulin	6	EEQIAEFKEAFSLF	**D**	-	K	**D**	G	**D**	-	G	**T**	**I**	TTK**E**	LGTVMRSL	GQNPT
12	parvalbumin	40	LDDVKKAFYVI	**D**	-	Q	**D**	K	**S**	-	G	**F**	**I**	**E**E**D**E	LKLFLQNF	SPSARALT
11	calpain EF1	98	EEERQFRKLFVQL	**A**	G	-	-	**D**	**D**	-	M	**E**	**V**	SAT**E**	LMNILNKVVT	RHPDLKTDGFG
12	calpain EF3	168	YLWNNIKKWQGIYKRF	**D**	-	T	**D**	R	**S**	-	G	**T**	**I**	GSN**E**	LPGAFEAA	GFHLN
14	ALG-2 EF5	156	IVLQRLTDIFRRY	**D**	T	-	**D**	Q	**D**	-	G	**W**	**I**	QVSYEQ	YLSMVF	
12	myosin RLC	14	QKQIQEMKEAFSMI	**D**	V	-	**D**	R	**D**	-	G	**F**	**V**	SKE**D**	IKAISEQ	LGRAPD
14	myosin ELC	6	DEIDDLKDVFELF	**D**	F	W	**D**	**G**	**R**	**D**	-	G	**A**	**V**	DAF**K**	LGDVCRC	LGINPR

The amino acids involved in Ca^{2+}-binding are in bold type and highlighted; those contributing the main-chain carbonyl oxygen as the Ca^{2+} ligand are underscored. Acidic residues are colored red and basic residues are colored blue. In most structures there is a water molecule in the $-X$ Ca^{2+}-coordinating position. The $-Y$ Ca^{2+}-ligand and the adjacent branched hydrophobic residue (highlighted in yellow) are those that form the key structure called EFβ-scaffold (cf. Figure 1). The EF-hand motifs in the upper part of the Table bind Ca^{2+} in a pentagonal bipyramid geometry. Note that the N-terminal part of the Ca^{2+}-binding loop may have different length, and either the main-chain carbonyl or the side-chain carboxyl oxygen atoms can be involved in Ca^{2+} coordination, as indicated. The ligand in the $-Y$ position is always the main-chain carbonyl oxygen. The C-terminal part of the loop is invariant in length. The last ligand spaced five residues C-terminal to the $-Y$ ligand is always a glutamate. Some exceptions to these rules shown in the bottom part of the Table lead to a different Ca^{2+}-coordination. The myosin light chains shown are those of scallop myosin.[49] The first EF-hand of the regulatory light chain in 1WDC contains Mg^{2+} rather then Ca^{2+}.

insertion of two residues after the first ligand, which enables Ca^{2+}-coordination entirely by the N-terminal part of the loop.[49] In the apoptosis-linked gene-2 (ALG-2), a member of the calpain family, an insertion of two amino acids in the C-terminal part of the Ca^{2+}-binding loop in EF-hand V leads to the octahedral Ca^{2+}-coordination involving only the N-terminal part of the loop.[43]

The important conclusion from the above discussion is that there is a clear distinction between the N and C-terminal parts of the Ca^{2+}-binding loop. The N-terminal part is variable, and significant differences in the length and amino acid sequence, including substitutions of the residues in the Ca^{2+}-liganding positions, can be accommodated without affecting the pentagonal bipyramid Ca^{2+}-ligand geometry. In contrast, the C-terminal part of the loop is constant and the amino acid sequence spacing between the $-Y$ and $-Z$ ligands is conserved. The distinction between the two parts of the Ca^{2+}-binding loop is paralleled and strongly emphasized by the differences in their structure and dynamics. In the absence of Ca^{2+} the N-terminal part of the loop is poorly structured and very dynamic, as evidenced by NMR[16,50,51] and by very high backbone temperature factors in the crystal structures[52] (cf. also Figure 6 of Grabarek[37]). The C-terminal part of the loop is highly structured with or without Ca^{2+}. It is stabilized by strong hydrogen bonds to the Ca^{2+}-binding loop of the pair-mate EF-hand. Furthermore, the last three residues of the loop form the first turn of the exiting helix and are stabilized by the α-helical $i, i+4$ backbone hydrogen bonds (reviewed by Strynadka & James[21]). These differences have strong implications with respect to the Ca^{2+}-binding mechanism (see below).

The Two-EF-hand Domain as a Functional Unit

The EF-hand motifs always occur in pairs. The structural integrity of the two-EF-hand domain is maintained by the backbone hydrogen bonds connecting the Ca^{2+}-binding loops in a short stretch of antiparallel β-sheet, and by numerous hydrophobic contacts between the helices.[21,53] In the Ca^{2+}-bound form the domain is further stabilized by the Ca^{2+}-ligand interactions and by a network of hydrogen bonds between polar groups and tightly bound water molecules (for a review, see Strynadka & James[21]). The two EF-hands in the domain are related by an approximate 2-fold symmetry axis; however, they are not identical. In fact, the EF-hand's position in a pair is strictly defined and has been designated as either "odd" or "even".[54] Using single EF-hand synthetic peptides corresponding to site III and site IV of troponin C, Shaw *et al.* demonstrated that a heterodimer is formed preferentially, and is much more stable than either one of the homodimers.[55,56] Similar observations have been reported for calbindin D9k.[57] These studies indicate that specific contacts between the helices make a critical contribution to the domain stability. However, the looploop interaction persists even in the absence of any stabilization from the helical segments, as demonstrated by Wojcik *et al.*[58] who found that a 12-residue synthetic

peptide analog of the Ca^{2+}-binding site III of calmodulin binds Tb^{3+} cooperatively and forms a well-structured dimer.

The smallest EF-hand protein, calbindin D9k, and the S100 proteins have a 14-residue loop EF-hand in the odd position paired with a 12-residue loop EF-hand. There is a large group of proteins containing two pairs of EF-hand motifs; the universal Ca^{2+}-regulator calmodulin (CaM) and troponin C (TnC) belong to this category. There are also Ca^{2+}-binding proteins containing six, eight or even 12 EF-hand motifs. The pairing principle is seemingly abandoned in the tri-EF-hand (parvalbumin, oncomodulin) and penta-EF-hand proteins (grancalcin, calpain, ALG-2). However, in the unpaired AB site of parvalbumins several characteristic features of the EF-hand motif are absent. This site does not bind Ca^{2+} and simply stabilizes the functional (CD/EF) pair.[59] Substitution of a canonical 12-residue Ca^{2+}-binding loop for the inactive loop does not restore the Ca^{2+}-binding properties to this site and causes overall destabilization of the structure.[60] Thus, despite the apparent evolutionary relationship to other EF-hand motifs[61] the AB site in parvalbumins should not, perhaps, be considered an EF-hand. In the penta-EF-hand proteins two molecules form a dimer through the fifth EF-hand, thus the interactions typical for the two-EF-hand domain are preserved.[40,42,43]

The EF-hand pairing principle has some important functional consequences. The structure connecting the Ca^{2+}-binding loops plays the key role in the Ca^{2+}-binding mechanism and in the Ca^{2+}-induced conformation change (see below). It also contributes to the fine-tuning of the Ca^{2+}-binding affinity and cooperativity.[24,26] By combining EF-hand motifs having different characteristics, domains with highly specialized conformational response and target specificity have evolved. The diversity of structural forms in EF-hand proteins is greatly expanded by the various types of domain–domain interactions (for a review, see Nelson & Chazin[12]). In both TnC and CaM the N and C-terminal domains are structurally independent, the property first demonstrated by proteolytic digestion[62–64] and explained by the respective crystal structures.[65–67] However, the functional significance of domain independence is different in these two proteins. In the case of TnC, which interacts with only two proteins, troponin I and troponin T, the N-terminal domain functions as the Ca^{2+}-specific regulatory switch, while the C-terminal domain plays mainly the structure stabilizing role.[68–71] In the case of CaM, domain independence is the key to the extreme versatility of this protein.[35] The two domains of CaM can converge on a short target sequence, e.g. the myosin light chain kinase,[29,72–74] or may interact independently of each other with distant regions of the target molecule, as is the case for anthrax adenylate cyclase.[75] Furthermore, there is a group of targets (utilizing the so-called IQ-motif) that have a preference for the apo form of CaM[31,33] with the domains in close contact, or positioned at some distance.[76] In contrast to CaM and TnC in other currently available EF-hand protein structures the relative disposition of the domains is fixed by intra- and/or intermolecular contacts. In the S100 proteins the domain–domain interactions occur through homo- or hetero-dimerization.[77–81] A compact arrangement of four EF-hands reminiscent of parvalbumins is found in the invertebrate sarcoplasmic calcium-binding proteins.[82,83] In recoverin[84,86] and related four EF-hand proteins from the group termed neuronal calcium sensors (NCS) including frequenin,[87,88] calcineurin B,[89] CIB1,[46] KChIP1[47] the domains are positioned sideways with respect to each other, which creates an extensive hydrophobic surface. In the penta-EF-hand proteins of calpain family (calpain,[40,41] grancalcin,[42] ALG-2[43]) a complex molecular structure is generated by a combination of compact intramolecular domain packing and intermolecular interactions within a dimer. There appear to be countless options for complex inter-domain interactions within the polypeptide chains composed entirely of EF-hand motifs, or multi-domain proteins containing a combination of EF-hand domains and other domains such as kinase, phosphatase, nuclear transport signal sequences, etc.

The Ca^{2+}-induced Conformational Change

The key attribute of the regulatory EF-hand proteins is the ability to change their conformation upon binding Ca^{2+}, thus acquiring different interactive properties. In the original crystal structure of TnC[65,66] Ca^{2+} is bound only to the C-terminal domain, which presents an open conformation with a large, solvent-exposed hydrophobic pocket. The Ca^{2+}-free N-terminal domain has a closed conformation in which all helices are tightly packed against each other. Herzberg *et al.*[90] proposed that Ca^{2+}-binding causes a transition from the closed to the open domain conformation, in which the exposed hydrophobic pocket serves as a target interaction site. This proposal known as the HMJ model has been supported by biochemical[91–93] and structural data.[94–97] It was also found applicable to calmodulin.[50,51,98–100] However, owing to insufficient structural information, it is unclear how widespread this type of a conformational change is among the EF-hand proteins.

A very different conformational change occurs in S100 proteins. The structure of EF-hand I of calcyclin (S100A6) determined by X-ray crystallography is very similar in the apo and in the Ca^{2+}-bound states.[79] In contrast, in EF-hand II Ca^{2+} induces a large 86° change in the orientation of helix III with respect to helix IV. Somewhat surprisingly, this change was not initially detected by NMR,[101] however, it became apparent in the refined structure.[81] A large Ca^{2+}-dependent change in the orientation of helix III was also found in S110B[102–107]

and based on the respective apo structures it most likely occurs also in S100A1[108] and S100A3.[109] This reorientation of helix III results in the formation of a hydrophobic patch surrounded be a number of acidic residues in the S100 dimer, which is proposed to function as the target recognition site. The exceptionally large change in the position of helix III is related, at least in part, to the "inverted" conformation of the Ca^{2+}-binding loop II in the apo structure. Irrespective of the actual mechanism, the most remarkable feature of the Ca^{2+}-induced conformational change in S100 proteins is the independent movement of the helices, which is in stark contrast to the concerted action of the EF-hands in TnC and CaM. A corollary to this observation is the conclusion that there must be a significant flexibility in the inter-helical interactions in the two-EF-hand domain. It seems plausible that owing to the structure stabilizing effect of the bound Ca^{2+}, the range of acceptable helix–helix orientations in EF-hand proteins may be broader than those generally found in proteins and theoretically predicted by the knobs-in-holes model by Crick[110] or the ridges-in-grooves definition by Chothia *et al*.[111,112]

Structural and biochemical evidence indicate that some EF-hand proteins do not change conformation upon Ca^{2+}-binding, which appears to preclude their Ca^{2+}-dependent regulatory function. Such "non-sensor" proteins (e.g. calbindin D9k and possibly parvalbumins) have been proposed to work as Ca^{2+}-buffers, thus indirectly contributing to Ca^{2+} regulation by modulating the shape and/or duration of Ca^{2+} signals.[12–114] To explain the difference in Ca^{2+}-response between the sensor and non-sensor EF-hand proteins, Nelson & Chazin considered the energy balance mechanism.[53] They suggested that CaM and other Ca^{2+}-sensor proteins adopt the open conformation because the geometric strain caused by binding Ca^{2+} in the closed domain conformation is energetically more costly than the exposure of hydrophobic side-chains in the open conformation. In the non-sensor EF-hand proteins, the energy balance was presumed to shift the equilibrium towards the closed conformation. Undoubtedly, the energy balance plays an important role by linking the domain opening to the Ca^{2+} and target binding. For example in cardiac TnC, in which site I does not bind Ca^{2+}, the N-terminal domain remains closed upon Ca^{2+} binding to the single active site II.[115,116] It does open, however, in the presence of the target molecule, troponin I,[117] or the calcium sensitizing drug, bepridil.[118] Similarly, in the mutant of skeletal TnC in which site I is disabled by substitution of Ala for the bidentate ligand, Glu41, the open domain conformation is observed only when both Ca^{2+} and the target peptide are bound.[119,120] A substitution of hydrophobic amino acids for Gln41 and Lys75 at the interface between the B/C linker and helix D in the N-terminal domain of CaM was shown to stabilize the closed domain conformation and decrease the Ca^{2+}-affinity.[121,122] It has been pointed out that CaM and TnC contain an unusually large number of methionine residues, whose side-chains become exposed to solvent in the Ca^{2+}-bound conformation. This could account for a smaller energy loss in these proteins upon domain opening, because sulfur atoms have higher polarizability than carbon atoms, thus are less hydrophobic.[53,123] To test this hypothesis Zhang *et al*.[124] substituted Leu for various Met residues in CaM. They found that the mutations impair CaM's ability to activate phosphodiesterase, but the location of the mutated sites appears to be more important than the overall number of substituted methionine residues. In another work, a substitution of up to 90% of Met in CaM with norleucine (a sulfur-free homolog of methionine) caused only a 10% decrease in CaM's ability to activate the myosin light chain kinase and had no effect on the overall structure, as judged by NMR.[125] In the effort to re-engineer calbindin D9k Bunick *et al*.[126] have introduced four Met residues among the 15 mutated interhelical contact sites. The mutant protein, named calbindomodulin, showed increased conformational sensitivity to Ca^{2+}, but failed to mimic the intended large Ca^{2+}-induced conformation change characteristic of CaM.[126] These studies do not address directly the question of the exact contribution of Met side-chains to the energy balance, but they indicate that there is little correlation between Met content and the Ca^{2+}-induced domain opening.

While many observations are consistent with the energy balance mechanism, several questions remain unanswered. What are the structural features of the sensor EF-hand proteins that cause the hypothetical "geometric strain"? Is the Ca^{2+}-binding to the non-sensor proteins accomplished with less or no strain? How large is the energy loss due to the breaking of the interhelical contacts? Can we assess these factors from the amino acid sequence of the EF-hand, and ultimately predict the conformational response? A closer look at the conformational changes in various EF-hand proteins may provide some answers.

The conformation of an EF-hand is often characterized by the interhelical angle, i.e. the angle between vectors defined by the averaged positions of the 11 backbone atoms at the N and C termini of the respective helices. Accordingly, the Ca^{2+}-induced conformational change in TnC and CaM can be described as a decrease in the EF-hand interhelical angle from $\sim$135° (approximately antiparallel) to $\sim$90° (approximately perpendicular). Nelson & Chazin[53] obtained a much more detailed description of the conformational changes in TnC and CaM with the use of distance difference matrix analysis. With their approach, the critical interhelical contacts and their changes are readily identified. More importantly, the changes within each EF-hand can be interpreted in the context of the entire domain. They have shown that while the interhelical angle between the two exiting helices (helix II and helix IV in the two-EF-hand domain) does not change upon Ca^{2+}-binding, their distance increases significantly, making an important contribution to the formation of the hydrophobic cleft. Another important observation from their analysis

is that the tops of the helices in each EF-hand (the ends close to the Ca^{2+}-binding loop) are slightly closer together in the Ca^{2+}-loaded state, while the bottoms are farther apart.[53] This observation is consistent with the Ca^{2+}-binding loop being more compact in the Ca^{2+}-bound state.[52,97] In a different approach proposed by Yap *et al.*[127] the position of the exiting helix of an EF-hand is described by a three-angle rotation and an offset with respect to the incoming helix. Using this method Yap *et al.* have analyzed the X-ray crystallographic and NMR structures of 90 EF-hands in 31 proteins and concluded that EF-hand motifs display a multitude of unique conformational states, together constituting a conformational continuum.[127] Also a broad distribution of interhelical angles was found in the most recent analysis of a large database containing 307 two-EF-hand domains.[128] These observations underscore the exceptional structural versatility of the EF-hand motif, which apparently has the capacity to function in a very broad conformational landscape.

The Ca^{2+}-binding Mechanism

The HMJ model and the more recent analytical methods discussed above describe the Ca^{2+}-induced conformational change, but they do not explain the underlying mechanism. It is not clear why the Ca^{2+}-coordination by the EF-hand's ligands should require a change in the orientation of the helices, or why a conformational strain should occur if the helices do not move. It appears that it may be possible to answer these questions if, in addition to the Ca^{2+}-free and the Ca^{2+}-bound structures of an EF-hand protein, we also have some information about the intermediate state or states. Recently, the X-ray crystallographic structure of one such conformational intermediate became available for calmodulin.[37] A mutant (CaM41/75) having the N-terminal domain locked with a disulfide bond in the closed (apo-like) conformation was crystallized in the Ca^{2+}-bound state. The structure shows that in the locked domain Ca^{2+} interacts only with the N-terminal parts of the Ca^{2+}-binding loops, but the C-terminal Glu ligands (the $-Z$ position) are 2.0−3.6 Å farther than required for the oxygen–Ca^{2+} bond. This structure provided the evidence that the conformational change in CaM is directly coupled to the proximity of the bidentate Glu ligand to the Ca^{2+}. A similar conclusion was reached for TnC by Gagne *et al.*[119] based on the NMR structure of the E41A mutant of TnC. It is also consistent with the biochemical data showing that CaM having the bidentate Glu ligand mutated has impaired Ca^{2+}-binding and target interaction properties.[129–131]

Despite the "incomplete" coordination and the closed domain conformation, the two Ca^{2+} in the locked N-domain of CaM41/75 were found to be at the same distance from each other as in the native, Ca^{2+}-bound, open-domain structure (Figure 1(a)). This observation led to the conclusion that the

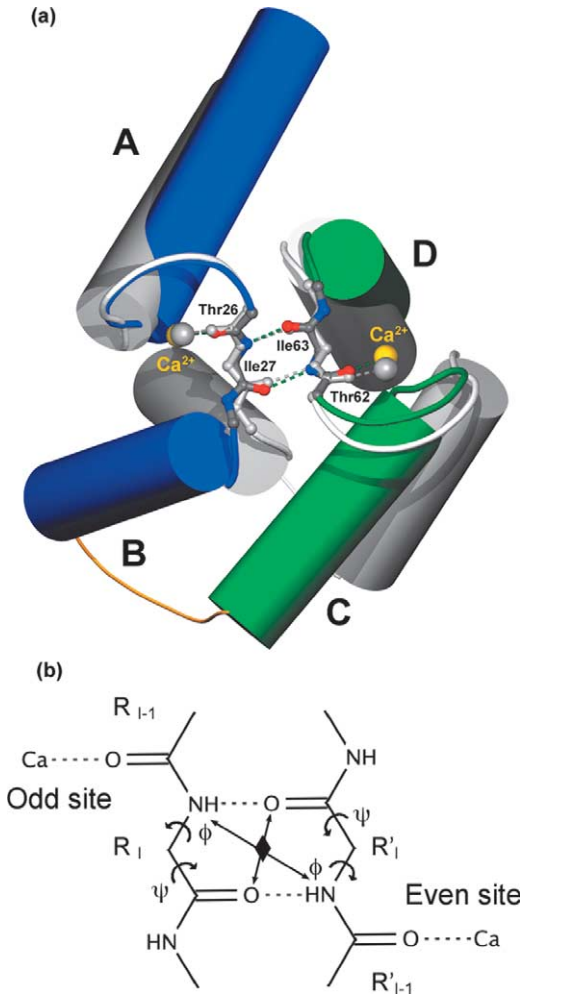

Figure 1. The EF-hand β-scaffold. (a) Comparison of the N-terminal domain of CaM in the Ca^{2+}-bound open conformation (PDB code 1CLL) with the Ca^{2+}-bound closed intermediate structure of CaM41/75 (PDB code 1Y6W). The EF-hand I of the native CaM is shown in blue and the EF-hand II in green. The structure of CaM41/75 is shown in gray. For superimposition of the two structures the backbone atoms of Thr26, Ile27, Thr62 and Ile63 were used (RMSD = 0.36 Å for 16 atoms). These atoms form the structure referred to as the EF-hand β-scaffold. (b) Schematic representation of the EF-hand β-scaffold. The Ca^{2+} binding loops are connected by two hydrogen bonds between the centrally located branched hydrophobic residues R_I (Ile27 in EF-hand I of CaM) and R'_I (Ile63 in EF-hand II of CaM). The carbonyl oxygen atoms of residues R_{I-1} and R'_{I-1} are the invariant Ca^{2+}-ligands. The distance between the bound Ca^{2+} is strictly defined by the bond network, as shown. Changes in the backbone ϕ, ψ angles of R_I and R'_I in the directions shown by the arrows enable the last ligand, the glutamate side-chain in R_{I+4} position to move into the Ca^{2+}-coordinating position, thus closing the Ca^{2+}-binding loop. The black diamond indicates an approximate 2-fold symmetry axis relating the odd and even EF-hands in the domain structure and it coincides with the Z axis of the local frame of reference used for structure comparison in Figure 3. The directions of the O- and N-axes of that frame of reference are indicated by the arrows. This Figure and the molecular graphics in Figures 2 and 3 were prepared with the POVScript+[150] version of MOLSCRIPT [151] and rendered with POV-Ray (Persistence of Vision Raytracer PTy. Ltd).

position of the bound Ca^{2+} in the two-EF-hand domain does not change during the domain opening and is defined primarily by the bond network involving the invariant carbonyl oxygen ligand in the center of the Ca^{2+}-binding loop and the two hydrogen bonds of the adjacent Ile residue (a part of the short anti parallel β-sheet). In view of this structure's role in positioning the Ca^{2+}, this bond network was named EF-hand-β-scaffold (Figure 1(b)). The importance of this structure for the stabilization of the Ca^{2+}-bound conformation was also evident from the NMR studies and the quantum mechanics calculations of Biekofsky *et al*.[132–134] These authors pointed out that the positive charge of the bound Ca^{2+} polarizes the bond network connecting the loops and leads to the formation of a resonance structure, which as they concluded, stabilizes the Ca^{2+}-bound structure and may contribute to the Ca^{2+}-binding cooperativity.

The structure of CaM41/75 provided yet another key piece of information. It gave the opportunity to discern the changes in the backbone conformation caused by the Ca^{2+} binding from those directly related to the domain opening,[37] a distinction that could not be made from the earlier crystallographic studies.[96,97] A comparison of CaM41/75 with the wild-type CaM has shown that Ile27 and Ile63, the two residues of the EFβ-scaffold, are those that change the backbone conformation the most during the transition from the closed to the open domain conformation. In fact, the rotation of the N–C^{α} bond (φ angle) and the C^{α}–C bond (ψ angle) of Ile27 was shown to be sufficient for the exiting helix of EF-hand I to change its orientation and to bring the bidentate Glu ligand into the Ca^{2+} coordinating position.[37]

Based on the cumulative information discussed above a two-step Ca^{2+}-binding mechanism was proposed according to which the Ca^{2+} binds initially to the N-terminal part of the Ca^{2+}-binding loop (the mobile, variable part), thus generating a rigid link between the incoming helix and the EFβ-scaffold. In the second step, the backbone torsional flexibility in the EFβ-scaffold enables the exiting helix to change its orientation, so the bidentate Glu ligand can move into the Ca^{2+} coordinating position.[37] This model defines specifically the link between the Ca^{2+}-binding and the conformational change. The ∼2 Å shift of the bidentate Glu ligand that is required for closing the loop and completion of the Ca^{2+}-coordination sphere causes the exiting helix to move and drives the conformational change. In this mechanism the variable N-terminal and the constant C-terminal parts of the Ca^{2+}-binding loop play distinct and very specific roles. The N-terminal part immobilizes the Ca^{2+} and positions it for the interaction with the last ligand, while the precise movement of the C-terminal part drives the conformational change. This model is referred to as the EF-hand β-scaffold model (EFBS model).

In the EFBS model the incomplete Ca^{2+} binding involving only the N-terminal part of the loop is proposed to be the key intermediate state in the Ca^{2+}-binding process. In CaM41/75 this state was captured owing to the engineered disulfide bond. It will have to be determined experimentally how populated such an intermediate is in the kinetic pathway of the native protein and what is the interdependence of the transitions in the two EF-hands of the domain. However, there are at least two other structures in the Protein Data Bank featuring a very similar mode of Ca^{2+}-binding, thus providing support for the idea that the N-terminal part of the loop is capable of Ca^{2+} binding independently of the C-terminal part. One example is the fifth EF-hand of ALG-2 (PDB code 1HQV), in which a two amino acid insertion in the C-terminal part of the loop and a substitution of Gln for the C-terminal Glu precludes the normal Ca^{2+} binding.[43] Another example is the first EF-hand of the essential light chain of Physarum myosin II[135] (PDB code 2BLO). In this structure, like in CaM41/75, a water molecule binds in the place of the bidentate Glu ligand, and the Ca^{2+}-coordination is octahedral. It appears that Ca^{2+}-binding is arrested at this step when some structural constraints prevent the movement of the exiting helix that brings the C-terminal Glu ligand into the Ca^{2+}-coordinating position.

Torsional Flexibility of the EFβ-scaffold

The effect of backbone torsional flexibility in the EFβ-scaffold on the EF-hand conformation requires further consideration. For this, rigid-body type modeling was performed using the EF-hand I of CaM41/75 as a model. The backbone φ,ψ angles of Ile27 were changed in small increments, while monitoring the interhelical angle and the proximity between the $-Y$ ligand and the $-Z$ ligand (the Thr26 O–Glu31 C^{β} distance). As shown in Figure 2, a change in the interhelical angle as large as 80°, and up to 2.5 Å shift in the position of Glu31 can be generated by adjusting the backbone conformation in Ile27 within the permitted range of φ,ψ angles. It is clear that various combinations of φ,ψ angles in Ile27 may generate the same interhelical angle. Most importantly, orientations of the exiting helix differing by as much as 30° may be compatible with Glu31 being in the Ca^{2+}-coordinating position, which corresponds to the Thr26 O–Glu31 C^{β} distance of ∼5.6 Å (the shaded area in the graph, Figure 2). Similar results were obtained when the coordinates of the Ca^{2+}-bound wild-type CaM were used for the calculations; however, the corresponding φ,ψ graphs were shifted on the ψ axis by approximately 20° (data not shown). This difference appears to reflect a contribution from bond rotation in another residue(s) in the C-terminal part of the loop, most likely Thr28, which is least constrained. As previously noted[37] bond rotation in Thr28 alone does not bring Glu31 sufficiently close to the bound Ca^{2+}, but it may be involved in fine-tuning of the conformational

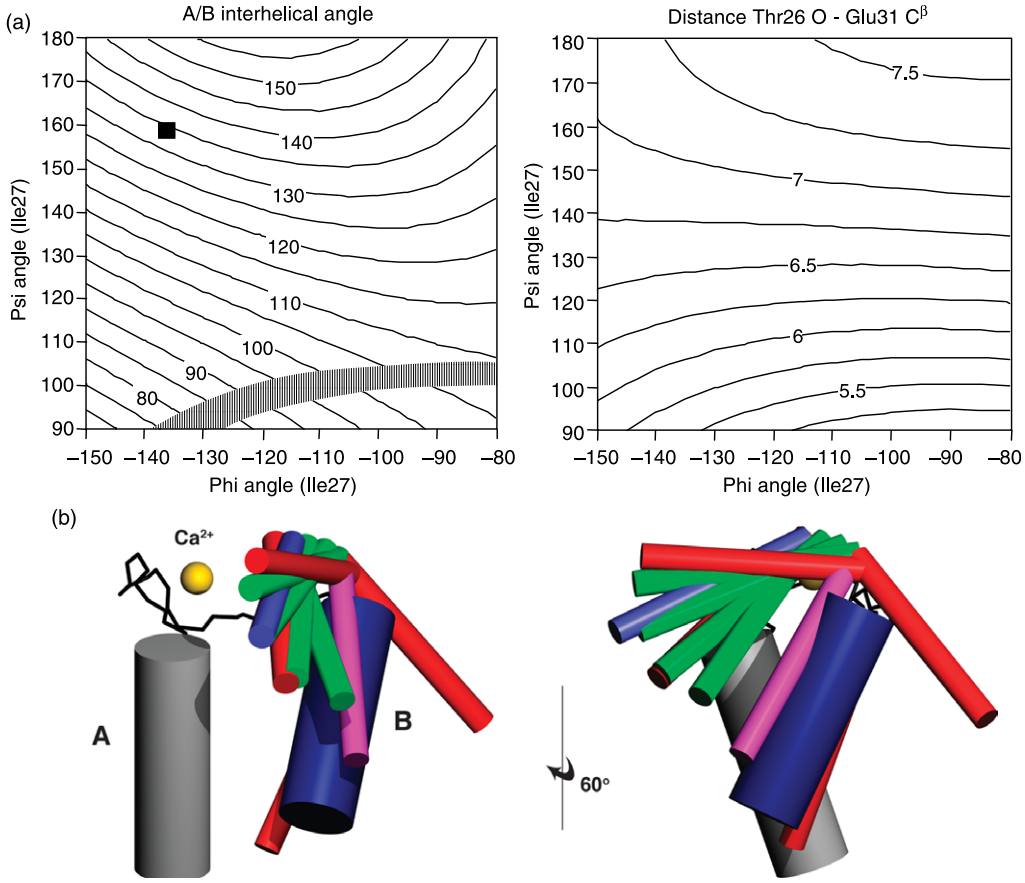

Figure 2. Effect of bond rotation in Ile27 on the structure of EF-hand I of CaM. The coordinates of CaM41/75 (closed conformation with bound Ca^{2+}, PDB code 1Y6W) were used for the calculations. The ϕ,ψ angles of Ile27 were systematically adjusted in 5° increments allowing the C-terminal part of the polypeptide chain to rotate. A dedicated script (courtesy of Eric Pettersen) and the program UCSF Chimera[144] were used for the calculations. (a) Plots of the interhelical angles (calculated with the program interhlx, provided by Kyoko Yap, University of Toronto) and the Thr26 O–Glu31 C^{β} distances as a function of Ile27 ϕ,ψ angles. The black square indicates the initial ϕ,ψ values and the shaded area indicates the approximate range of the conformations that are consistent with the C-terminal glutamate ligand being in the Ca^{2+}-coordinating position (the Thr26 O–Glu31 C^{β} distance ~5.6 Å). (b) Graphical representation of selected conformations are shown in two orientations related by 60° rotation around *Y* axis. All structures have been superimposed using the C^{α} atoms of residues 10–27. The thick cylinders represent the starting conformation (1Y6W), which is similar to the closed apo structure (1QX5). The four green cylinders show the conformations corresponding to the shaded area of the ϕ,ψ plot. The thin blue cylinder represents the Ca^{2+}-bound open conformation (1CLL). The red cylinders show the conformers corresponding to the ϕ,ψ values in the four corners of the plot, and the magenta cylinder represents the center of the plot (ϕ = −115°, ψ = 135°). Note that the geometrical properties of the EF-hand are tested only. While all tested ϕ,ψ values are within the allowed region of the Ramachandran plot, the actual conformational space is restricted by the inter-atomic contacts and the overall folding energy, which were not considered here.

change, consistent with the conclusion reached by Strynadka *et al.* for the N-terminal domain of TnC.[97]

The conclusion from this analysis is that the EFβ-scaffold provides a very versatile hinge in the EF-hand that enables the C-terminal ligand to move into the Ca^{2+}-coordinating position, thus closing the coordination sphere of the Ca^{2+} and changing the relative orientation of the helices. This way various structural responses can be achieved. Naturally, in the context of the two-EF-hand domain structure the movement of the helices is restricted by the inter-helical contacts and by the overall folding energy. These limitations were not considered here, thus the actual conformational space accessible to the protein may not be as broad as implied by Figure 2. On the other hand, there is evidence suggesting that the domain structure of the Ca^{2+}-bound CaM is quite dynamic and the protein may sample a broad range of conformations. Recently, Fallon & Quiocho[136] reported the crystal structure of the Ca^{2+}-bound bovine brain CaM in which the N-domain is only half as open as in other reported structures. Based on the small angle X-ray diffraction experiments and molecular dynamics simulations Vigil *et al.*[137] concluded that the N-terminal domain of CaM fluctuates in solution between closed and open conformations. They further suggested that the closed conformation is the dominant state in solution and the open conformation observed in the crystal structure results from stabilization by the crystal lattice. A generally similar view of a

dynamic domain in the Ca^{2+}-ligated state was presented by Chou *et al.*[18] on the basis of their NMR experiments. However, they excluded the possibility that the fully closed apo conformation is partially populated in the Ca^{2+}-ligated state. The conformational landscape accessible to the CaM domains also appears to be very broad under the conditions of low Ca^{2+} concentrations, under which only one of the Ca^{2+}-binding sites is filled.[16,17,138] Data in Figure 2 offer an explanation on how CaM may dynamically sample numerous conformations *via* changes to the ϕ,ψ torsional angles in the EFβ-scaffold, which dictate the different orientations of the helices until the appropriate conformation is adopted for specific target interaction.

Loop Closing *versus* Domain Opening in EF-hand Proteins

Are the Ca^{2+}-dependent changes in the EFβ-scaffold specific to the Ca^{2+}-sensor proteins? To answer this question the structures of calcyclin, osteonectin, calmodulin and calpain are compared and the key parameters are listed in Table 2. In all the analyzed EF-hands, irrespective of the loop length, Ca^{2+}-binding changes the ϕ,ψ angles of the central residue in the EFβ-scaffold and decreases the distance between the $-Y$ and $-Z$ ligands. These changes are consistent with the closing of the Ca^{2+}-binding loop similar to that found for the N-terminal domain of TnC.[52,97] However, changes in the interhelical angle vary greatly. Whereas there is a ∼40° change in CaM, there is only a modest change of 18° in calpain and almost no change in calcyclin. Thus, consistent with the data in Figure 2, the Ca^{2+}-binding loop can close with little or no change in the interhelical angle. The end point of the conformational change is reached when the oxygen atoms of the bidentate Glu ligand are 2.4 Å from the Ca^{2+} (corresponding to ∼5.6 Å distance between R_{I-1}-O and R_{I+4}-C^{β}), and are aligned with the equatorial plane of the Ca^{2+}–ligand complex. A range of values for the ϕ,ψ angles of the R_I residue can fulfill this requirement (Figure 2). It appears that the closing of the Ca^{2+}-binding loop enabled by the bond rotation in the EFβ-scaffold occurs in all EF-hands, but it may or may not lead to a significant change in the interhelical angle.

An important question is why do the Ca^{2+}-binding loops default to the open conformation in the absence of Ca^{2+}, especially in the proteins that do not change the domain conformation upon Ca^{2+}-binding. One reason appears to be the β-sheet structure connecting the Ca^{2+}-binding loops. In the apo form the open loop structure enables the formation of two additional hydrogen bonds between the carbonyl oxygen of the residue in the R_{I-2} position (frequently a Gly residue) and the amide nitrogen of the residue in the R'_{I+2} position of the pair-mate Ca^{2+}-binding loop. In the Ca^{2+}-bound, closed loop conformation these hydrogen bonds are broken, or replaced by weaker indirect hydrogen bonds through a water molecule. The electrostatic repulsion among the negatively charged side-chains may also contribute to the stabilization of the open loop conformation in the absence of Ca^{2+}.

Table 2. Effect of Ca^{2+} on the conformation of various EF-hand motifs

	Odd position				Even position			
Protein	ϕ Angle[a]	ψ Angle[a]	Distance[b]	E/F angle	ϕ Angle[a]	ψ Angle[a]	Distance[b]	E/F angle
Calmodulin, apo (8)[c]	−137±7.6	157±4.7	6.8±0.22	135±0.7	−146±3.3	137±4.5	7.1±0.11	128±1.1
$+Ca^{2+}$(5)	−109±2.4	125±1.1	5.64±0.04	92.6±1.5	−108±1.9	125±1.9	5.66±0.05	89.2±1.1
Calcyclin, apo (2)	−146	154	7.1	128	−133	129	6.1	158
$+Ca^{2+}$(3)	−97	124	5.4	136	−111	110	5.5	119
Calpain, apo (2)								
EF1,2	−106	156	6.6	144	−105	124	6.6	123
EF3,4	−112	138	7.0	145	−126	135	6.9	136
Calpain, $+Ca^{2+}$ (2)								
EF1,2	−91	113	5.6	126	−96	117	5.5	119
EF3,4	−106	113	5.7	136	(−114)[d]	(135)[d]	(6.8)[d]	(136)[d]
Osteonectin, $+Ca^{2+}$(1)	−120	118	5.5	117	−109	115	5.7	111

Structures used for the calculations: apo CaM,[145] 1QX5 (2.54 Å resolution), listed are the mean±standard error values calculated for the eight independently refined monomers; $+Ca^{2+}$-CaM, mean values±standard error calculated for five structures, 1CLL[146] (1.7 Å) human recombinant, 1OSA[147] (1.68 Å) paramecium recombinant, 1UP5[148] (1.9 Å) chicken gizzard, two monomers, 1RFJ[149] (2.0 Å) potato, recombinant; apo S100A6 (calcyclin) 1K9P[79] (1.9 Å), 1K8U[79] (1.15 Å);$+Ca^{2+}$-S100A6 1K96[79] (1.44 Å), 1K9K[79] (1.76 Å), two monomers; apo calpain, 1AJ5[40] (2.3 Å) and $+Ca^{2+}$-calpain, 1DVI[40] (2.3 Å), small regulatory subunit, domain VI, residues 87–270 of rat liver recombinant calpain, each containing two monomers; $+Ca^{2+}$-osteonectin (BM-40), 1SRA[44] (2.0 Å) recombinant carboxy-terminal domain (residues 136–286) of human extracellular matrix calcium binding protein SPARC/osteonectin. This structure was included owing to its unique 13 amino acid residue Ca^{2+}-binding loop; however, only the Ca^{2+}-bound structure of this protein is available.

[a] The ϕ,ψ backbone dihedral angles of the branched hydrophobic residue in the center of the loop (labeled R_I or R'_I in Figure 1(b)).

[b] The distance (Å) between C^{β} of the glutamate in the $-Z$ position and the Ca^{2+} ligand in the $-Y$ position (the invariant carbonyl oxygen ligand). This distance is affected only by the backbone conformation of the C-terminal part of the Ca^{2+}-binding loop and its decrease upon Ca^{2+}-binding reflects the closing of the loop.

[c] The number of structures used for the calculation. For CaM the mean values±standard error are listed. For all other structures the numbers are the mean values.

[d] The EF3 of calpain does not bind Ca^{2+}.

The EF-hand β-Scaffold as a Frame of Reference

Still unresolved is the question of the intrinsic structural features of the EF-hand motif that control domain opening. To address this question the structures of the EF-hand motifs having 11–14 amino acid residue Ca^{2+}-binding loops are compared in a local frame of reference defined by the EFβ-scaffold (Figure 3). In this view, it is clear that the Ca^{2+}-binding causes the exiting helix and the C-terminal Glu ligand to move, consistent with the data in Table 2. More importantly, some previously unrecognized features of the EF-hand structure become apparent. First, there are different orientations of the vector perpendicular to the plane of the five equatorial Ca^{2+} ligands. This vector points in a similar direction with respect to the EFβ-scaffold in calcyclin and calpain, but has a distinctly different orientation in CaM and osteonectin. The second difference is in the position of the incoming helix, which in calcyclin and calpain is approximately in line with the Ca^{2+}, whereas in CaM and osteonectin it is significantly offset towards the exiting helix. The origin of these differences becomes apparent if we consider the fact that the

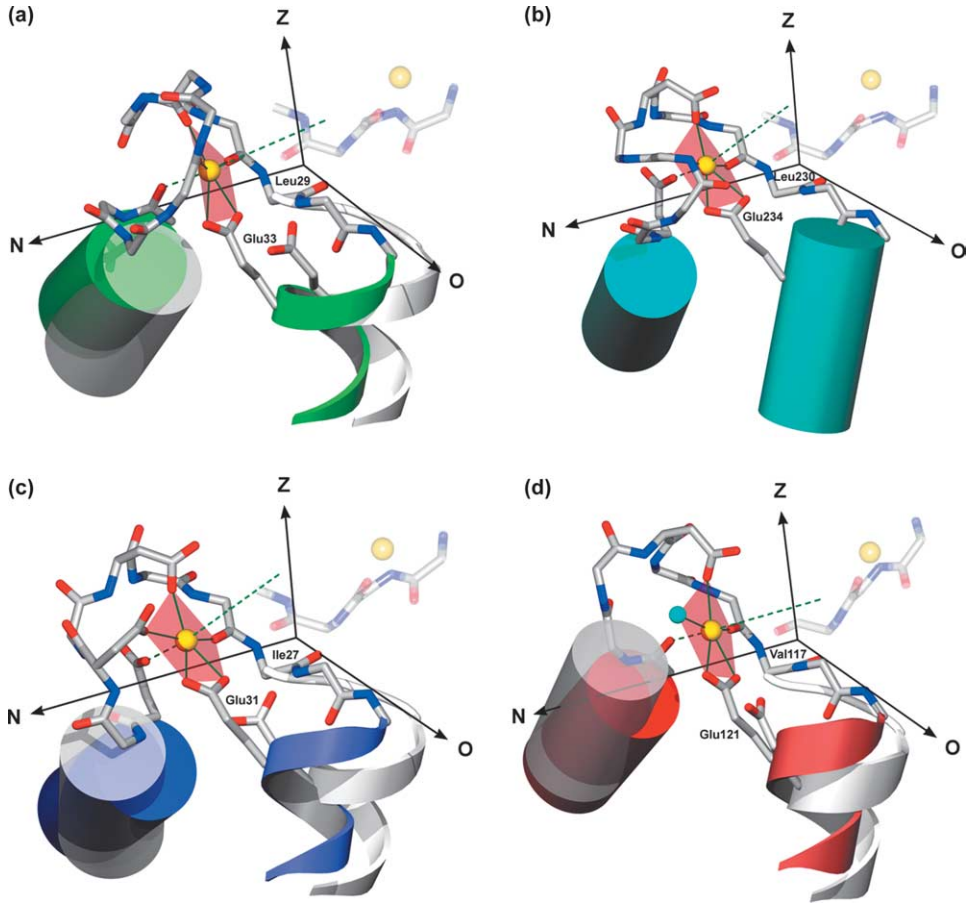

Figure 3. Comparison of various EF-hand motif structures in a conformation-independent frame of reference. Shown are the structures of the EF-hand motifs in the "odd" position in: (a) calcyclin (14 residue loop); (b) osteonectin (13 residue loop); (c) calmodulin (the canonical 12 residue loop); (d) calpain (11 residue loop). The amino acid sequences are listed in Table 1, and the PDB codes and references are in the legend to Table 2. The Ca^{2+}-bound structures are multicolored and the partial structures of the apo forms (where available) are shown in gray. The structures are shown in approximately the same orientation defined by the local frame of reference linked to the EFβ-scaffold. The backbone atoms of the EFβ-scaffold residues were used for the superimposition of the structures (RMSD range 0.29–0.43 for 16 atoms). The *N*-axis is defined by the vector connecting the nitrogen atom of the R_I residue with the nitrogen atom of the R_I' residue of the EFβ-scaffold; similarly the *O*-axis is defined by the carbonyl oxygen atoms in the same residues (cf. Figure 1(b)). The *Z*-axis is a vector perpendicular to the plane of the EFβ-scaffold calculated by approximating the position of the N and O atoms of the R_I and R_I' residues. The *Z*-axis coincides with the approximate non-crystallographic 2-fold symmetry axis of the domain. The *N*, *O*, *Z* coordinate system as defined above is approximately orthogonal, but depending on the exact position of the selected atoms (subject to structure refinement and the intrinsic protein dynamics) the axes may not intersect in one point. For simplicity of presentation the centroid of the EFβ-scaffold plane is used as the origin. Only a 1.5 turn short segment of each helix is shown. The Ca^{2+}-ligands positioned in the equatorial plane of the pentagonal bipyramid are connected by semitransparent surface and the vector normal to that plane is shown (the broken green line). For vector calculations the program Mathematica 5.0 (Wolfram Research, Inc.) was used.

position of the bound Ca^{2+} is fixed by the EFβ-scaffold. If that is the case, than the position of the C terminus of the incoming helix is also defined and depends on the first ligand of the loop (the X position). When the first ligand is an aspartate side-chain carboxyl (as in CaM and osteonectin), the incoming helix is shifted with respect to the Ca^{2+} by the distance equivalent to the side-chain's length. The consequence of this shift is that the C-terminal glutamate ligand has a more difficult access to the immobilized Ca^{2+}; it has to "reach over the top" of the incoming helix, which requires the exiting helix to pivot. The C terminus of the incoming helix, in particular the residue immediately preceding the first ligand, which in the odd EF-hands is often a bulky phenylalanine, becomes the pivoting point for the exiting helix. In contrast, in the EF-hands utilizing the main-chain carbonyl oxygen as the first ligand (e.g. calcyclin and calpain) the bidentate glutamate ligand has an unobstructed access to the immobilized Ca^{2+} and a simple rotation of the exiting helix is sufficient to bring this ligand into the Ca^{2+}-coordinating position. The key conclusion from this comparison is that the first ligand of the Ca^{2+}-binding loop is one of the main structural determinants of the exiting helix orientation and consequently of the extent of domain opening. One may predict that the EF-hands that employ an Asp side-chain as the first ligand will have an intrinsic preference for a change in the interhelical angle leading to the domain opening, whereas those employing the main-chain carbonyl as the first ligand will tend to remain in the closed conformation. It is important to keep in mind that the Ca^{2+}-induced response of each individual EF-hand is modified by the response of its pair-mate and the overall energy balance has a decisive role, as discussed earlier. By combining different types of EF-hand motifs in a domain a versatile mechanism has evolved for achieving a great variety of conformational responses tailored to specific functions.

Other Factors that Shape the Conformational Response

Stability of the exiting helix

The EFβ-scaffold concept clearly helps to explain how the stereo-specific requirements of the Ca^{2+}–ligand interactions shape the Ca^{2+}-binding loop and affects the position of the adjacent helices. However, owing to multiple contacts the helices are interlinked and a change in the position of one helix will inevitably affect the entire domain. The overall energetics of the domain may require that the integrity of individual helices be compromised. That is the case when one of the EF-hands in the domain is incapable of Ca^{2+} binding, or is predisposed to the closed domain conformation. The required closing of the Ca^{2+}-binding loop may occur without domain opening upon local

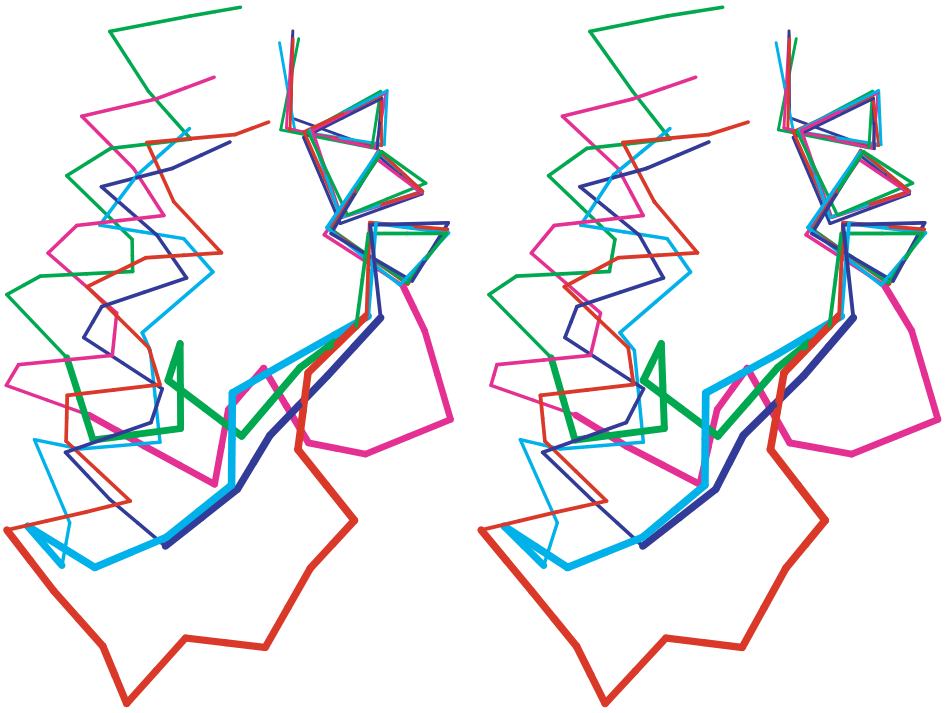

Figure 4. Variability in the linker connecting two EF-hand motifs in a domain. Shown in stereo are the C^{α} trace representations of the linker regions (thick line) and the adjacent helices (thin line) of: calcyclin (PDB code 1K96), green; calbindin D9k (3ICB), magenta; calmodulin site I,II (1CLL), blue; parvalbumin site II, III (1PVB), cyan; and calpain site I, II (1DVI), red. The structures were superimposed using the C^{α} atoms of the incoming helix from the EF-hand in the even position (on the right). The amino acid sequences of the segments defined as linkers are shown in Table 1.

distortion of the exiting helix. For example, the D helix in calbindin D9k has a regular α-helical conformation in the apo[139] and Mg^{2+}-bound forms,[140] but becomes distorted (a mixture of 3_{10} and α helix conformation) in the presence of Ca^{2+}.[39,141,142] In calpain, in which the fourth EF-hand is incapable of Ca^{2+}-binding, the exiting helix of its pair-mate (EF-hand 3) has a permanent kink, a Pro residue.[40] In these examples the distortion of the exiting helix and a loss of two hydrogen bonds is apparently less energetically costly than opening of the domain.

Significance of the B/C linker

In view of the requirement for the exiting helix (or part of it) to move in order to complete the Ca^{2+}-binding process, the relation of this helix to the incoming helix of the pair-mate EF-hand is important. The B/C linker appears to provide a mechanism for adjusting the relative position of these helices in the part of the domain that is most distant from the Ca^{2+}-binding site. It is interesting that CaM and TnC, the proteins that exhibit the largest domain opening among the EF-hand proteins, have the shortest B/C linkers. This appears to contribute to the strong coupling between the two helices, which facilitates their concerted movement during domain opening. As shown in Figure 4, the variability in the amino acid sequence and the length of the B/C linker (Table 1) is matched by the variability in its structure. In calcyclin and in other members of the S100 protein family the linker is exceptionally long and unusual in that it forms a 1.5 turn of an α-helix in the presence of Ca^{2+}. This contributes to the exceptional flexibility in the relative disposition of helix C with respect to helix B, which in turn enables a large change in the conformation of EF-hand II independent of EF-hand I.[79,106,107] The linker in S100 proteins also constitutes a part of the target-binding site in the dimeric form of the protein.[77,143]

Conclusions

The EFβ-scaffold concept proves to be useful in explaining the function of the EF-hand. The link between the Ca^{2+}-coordination by the protein ligands and the resultant conformational change can now be explicitly defined and readily interpreted in terms of the EF-hand β-scaffold's properties, i.e. the structural rigidity in the plane of the β-sheet and the torsional flexibility of the backbone. Hopefully, the theoretical framework outlined here will provide an inspiration for the design and interpretation of new experiments leading to a better understanding of the Ca^{2+}-dependent regulation.

The key premises of the proposed two-step model of the Ca^{2+}-binding mechanism, which appears to be applicable to all EF-hand proteins, can be summarized as follows.

(1) The Ca^{2+}-binding process and the resultant conformational changes in the two-EF-hand domain are controlled and enabled by the central structure named EFβ-scaffold, which defines the position of the bound Ca^{2+} and coordinates the function of the N-terminal (variable) and C-terminal (constant) parts of the Ca^{2+}-binding loop.
(2) The Ca^{2+} is immobilized initially by the EFβ-scaffold and the ligands of the N-terminal part of the Ca^{2+}-binding loop. The torsional flexibility of the EFβ-scaffold enables repositioning of the C-terminal part of the Ca^{2+}-binding loop together with the exiting helix, thus bringing the C-terminal bidentate Glu ligand into the Ca^{2+}-coordinating position.

Comparison of various EF-hand structures in a conformation-independent frame of reference linked to the EFβ-scaffold reveals differences suggesting that the nature of the ligand in the X position (the first ligand of the Ca^{2+}-binding loop) is the key structural determinant of the Ca^{2+}-induced conformational response. Those EF-hands that utilize the backbone carbonyl oxygen as the first ligand may have the intrinsic preference for the closed conformation while those employing the aspartate side-chain are likely to change the interhelical angle upon Ca^{2+}-binding. Other factors including some specific interhelical contacts, helix stability, the length, structure and flexibility of the linker segment, and the overall energy balance provide the fine-tuning of the conformational response in the two-EF-hand domain.

Finally, the model based on the EFβ-scaffold unifies the various modes of Ca^{2+}-binding to the EF-hand. The variability in the length and composition of the N-terminal part of the Ca^{2+}-binding loop is permitted, because the role of this part of the loop is to capture and immobilize the Ca^{2+} initially, which can be achieved in several different ways. The 11, 13 or 14 amino acid residue Ca^{2+}-binding loop EF-hands introduce diversity of structural design into the EF-hand family, while working on the same principle as the canonical EF-hand.

The two-EF-hand domain emerges as a versatile and dynamic structure. The right hand that R. H. Kretsinger elected over 30 years ago as a metaphor for the calcium-binding structural motif acquires new skills. While the palm of Kretsinger's EF-hand holds the Ca^{2+} firmly, the thumb and the index finger can move in many directions to perform highly specialized and precise work.

Acknowledgements

I thank James Fessenden, John Gergely, Krzysztof Grabarek, Knut Langsetmo, and C.- L. Albert Wang for critical comments on the manuscript. I am grateful to Eric Pettersen for writing the UCSF

Chimera script for incremental bond rotation and coordinates output.

References

1. Kretsinger, R. H. & Nockolds, C. E. (1973). Carp muscle calcium binding protein. II. Structure determination and general description. *J. Biol. Chem.* **248**, 3313–3326.
2. Collins, J. H., Potter, J. D., Horn, M. J., Wilshire, G. & Jackman, N. (1973). The amino acid sequence of rabbit skeletal muscle troponin C: gene replication and homology with calcium-binding proteins from carp and hake muscle. *FEBS Letters*, **36**, 268–272.
3. Collins, J. H. (1974). Homology of myosin light chains, troponin-C and parvalbumins deduced from comparison of their amino acid sequences. *Biochem. Biophys. Res. Commun.* **58**, 301–308.
4. Stevens, F. C., Walsh, M., Ho, H. C., Teo, T. S. & Wang, J. H. (1976). Comparison of calcium-binding proteins. Bovine heart and brain protein activators of cyclic nucleotide phosphodiesterase and rabbit skeletal muscle troponin C. *J. Biol. Chem.* **251**, 4495–4500.
5. Watterson, D. M., Harrelson, W. G., Jr, Keller, P. M., Sharief, F. & Vanaman, T. C. (1976). Structural similarities between the Ca^{2+}-dependent regulatory proteins of 3′:5′-cyclic nucleotide phosphodiesterase and actomyosin ATPase. *J. Biol. Chem.* **251**, 4501–4513.
6. Kawasaki, H. & Kretsinger, R. H. (1994). Calcium-binding proteins. 1: EF-hands. *Protein Profile*, **1**, 343–517.
7. Kawasaki, H. & Kretsinger, R. H. (1995). Calcium-binding proteins 1: EF-hands. *Protein Profile*, **2**, 297–490.
8. Berridge, M. J., Bootman, M. D. & Lipp, P. (1998). Calcium—a life and death signal. *Nature*, **395**, 645–648.
9. Berridge, M. J., Lipp, P. & Bootman, M. D. (2000). The versatility and universality of calcium signalling. *Nature Rev. Mol. Cell. Biol.* **1**, 11–21.
10. Carafoli, E., Santella, L., Branca, D. & Brini, M. (2001). Generation, control, and processing of cellular calcium signals. *Crit. Rev. Biochem. Mol. Biol.* **36**, 107–260.
11. Kahl, C. R. & Means, A. R. (2003). Regulation of cell cycle progression by calcium/calmodulin-dependent pathways. *Endocr. Rev.* **24**, 719–736.
12. Nelson, M. R. & Chazin, W. J. (1998). Structures of EF-hand Ca^{2+}-binding proteins: diversity in the organization, packing and response to Ca^{2+} binding. *Biometals*, **11**, 297–318.
13. Lewit-Bentley, A. & Rety, S. (2000). EF-hand calcium-binding proteins. *Curr. Opin. Struct. Biol.* **10**, 637–643.
14. Evenas, J., Thulin, E., Malmendal, A., Forsen, S. & Carlstrom, G. (1997). NMR studies of the E140Q mutant of the carboxy-terminal domain of calmodulin reveal global conformational exchange in the Ca^{2+}-saturated state. *Biochemistry*, **36**, 3448–3457.
15. Evenas, J., Malmendal, A., Thulin, E., Carlstrom, G. & Forsen, S. (1998). Ca^{2+} binding and conformational changes in a calmodulin domain. *Biochemistry*, **37**, 13744–13754.
16. Malmendal, A., Evenas, J., Forsen, S. & Akke, M. (1999). Structural dynamics in the C-terminal domain of calmodulin at low calcium levels. *J. Mol. Biol.* **293**, 883–899.
17. Evenas, J., Forsen, S., Malmendal, A. & Akke, M. (1999). Backbone dynamics and energetics of a calmodulin domain mutant exchanging between closed and open conformations. *J. Mol. Biol.* **289**, 603–617.
18. Chou, J. J., Li, S., Klee, C. B. & Bax, A. (2001). Solution structure of Ca^{2+}-calmodulin reveals flexible hand-like properties of its domains. *Nature Struct. Biol.* **8**, 990–997.
19. Chazin, W. J. (1995). Releasing the calcium trigger. *Nature Struct. Biol.* **2**, 707–710.
20. McPhalen, C. A., Strynadka, N. C. J. & James, M. N. G. (1991). Calcium-binding sites in proteins: a structural perspective. *Advan. Protein Chem.* **42**, 77–144.
21. Strynadka, N. C. J. & James, M. N. G. (1989). Crystal structures of the helix-loop-helix calcium-binding proteins. *Annu. Rev. Biochem.* **58**, 951–998.
22. Ikura, M. & Ames, J. B. (2006). Genetic polymorphism and protein conformational plasticity in the calmodulin superfamily: two ways to promote multifunctionality. *Proc. Natl Acad. Sci. USA*, **103**, 1159–1164.
23. Evenas, J., Malmendal, A. & Forsen, S. (1998). Calcium. *Curr. Opin. Chem. Biol.* **2**, 293–302.
24. Forsen, S., Linse, S., Drakenberg, T., Kordel, J., Akke, M., Sellers, P. *et al*. (1991). Ca^{2+} binding in proteins of the calmodulin superfamily: cooperativity, electrostatic contributions and molecular mechanisms. *CIBA Found. Symp.* **161**, 222–236.
25. Forsen, S. & Linse, S. (1995). Cooperativity: over the Hill. *Trends Biochem. Sci.* **20**, 495–497.
26. Linse, S. & Forsen, S. (1995). Determinants that govern high-affinity calcium binding. In *Advances in Second Messenger and Phosphoprotein Research* (Means, A. R., ed.), vol. 30, Raven Press, Ltd, New York.
27. Falke, J. J., Drake, S. K., Hazard, A. L. & Peersen, O. B. (1994). Molecular tuning of ion binding to calcium signaling proteins [Review]. *Quart. Rev. Biophys.* **27**, 219–290.
28. Haiech, J. & Kilhoffer, M. C. (2002). Deconvolution of calcium-binding curves. Facts and fantasies. *Methods Mol. Biol.* **173**, 25–42.
29. Crivici, A. & Ikura, M. (1995). Molecular and structural basis of target recognition by calmodulin. [Review]. *Annu. Rev. Biophys. Biomol. Struct.* **24**, 85–116.
30. Rhoads, A. R. & Friedberg, F. (1997). Sequence motifs for calmodulin recognition. *FASEB J.* **11**, 331–340.
31. Jurado, L. A., Chockalingam, P. S. & Jarrett, H. W. (1999). Apocalmodulin. *Physiol. Rev.* **79**, 661–682.
32. Hoeflich, K. P. & Ikura, M. (2002). Calmodulin in action: diversity in target recognition and activation mechanisms. *Cell*, **108**, 739–742.
33. Bahler, M. & Rhoads, A. (2002). Calmodulin signaling *via* the IQ motif. *FEBS Letters*, **513**, 107–113.
34. Bhattacharya, S., Bunick, C. G. & Chazin, W. J. (2004). Target selectivity in EF-hand calcium binding proteins. *Biochim. Biophys. Acta*, **1742**, 69–79.
35. Yamniuk, A. P. & Vogel, H. J. (2004). Calmodulin's flexibility allows for promiscuity in its interactions with target proteins and peptides. *Mol. Biotechnol.* **27**, 33–57.

36. Carafoli, E. & Klee, C. B. (1999). *Calcium as a Cellular Regulator*, Oxford University Press, New York, Oxford.
37. Grabarek, Z. (2005). Structure of a trapped intermediate of calmodulin: calcium regulation of EF-hand proteins from a new perspective. *J. Mol. Biol.* **346**, 1351–1366.
38. Szebenyi, D. M. E., Obendorf, S. K. & Moffat, K. (1981). Structure of vitamin D-dependent calcium-binding protein from bovine intestine. *Nature*, **294**, 327–332.
39. Szebenyi, D. M. E. & Moffat, K. (1986). The refined structure of vitamin D-dependent calcium-binding protein from bovine intestine. Molecular detail, ion binding, and implicaions for the structure of other calcium-binding proteins. *J. Biol. Chem.* **261**, 8761–8777.
40. Blanchard, H., Grochulski, P., Li, Y., Arthur, J. S., Davies, P. L., Elce, J. S. & Cygler, M. (1997). Structure of a calpain Ca^{2+}-binding domain reveals a novel EF-hand and Ca^{2+}-induced conformational changes. *Nature Struct. Biol.* **4**, 532–538.
41. Lin, G. D., Chattopadhyay, D., Maki, M., Wang, K. K., Carson, M., Jin, L. *et al*. (1997). Crystal structure of calcium bound domain VI of calpain at 1.9 A resolution and its role in enzyme assembly, regulation, and inhibitor binding. *Nature Struct. Biol.* **4**, 539–547.
42. Jia, J., Han, Q., Borregaard, N., Lollike, K. & Cygler, M. (2000). Crystal structure of human grancalcin, a member of the penta-EF-hand protein family. *J. Mol. Biol.* **300**, 1271–1281.
43. Jia, J., Tarabykina, S., Hansen, C., Berchtold, M. & Cygler, M. (2001). Structure of apoptosis-linked protein ALG-2: insights into Ca^{2+}-induced changes in penta-EF-hand proteins. *Structure (Camb)*, **9**, 267–275.
44. Hohenester, E., Maurer, P., Hohenadl, C., Timpl, R., Jansonius, J. N. & Engel, J. (1996). Structure of a novel extracellular Ca^{2+}-binding module in Bm-40. *Nature Struct. Biol.* **3**, 67–73.
45. Cates, M. S., Berry, M. B., Ho, E. L., Li, Q., Potter, J. D. & Phillips, G. N., Jr (1999). Metal-ion affinity and specificity in EF-hand proteins: coordination geometry and domain plasticity in parvalbumin. *Struct. Fold. Des.* **7**, 1269–1278.
46. Gentry, H. R., Singer, A. U., Betts, L., Yang, C., Ferrara, J. D., Sondek, J. & Parise, L. V. (2005). Structural and biochemical characterization of CIB1 delineates a new family of EF-hand-containing proteins. *J. Biol. Chem.* **280**, 8407–8415.
47. Scannevin, R. H., Wang, K., Jow, F., Megules, J., Kopsco, D. C., Edris, W. *et al*. (2004). Two N-terminal domains of Kv4 K(+) channels regulate binding to and modulation by KChIP1. *Neuron*, **41**, 587–598.
48. da Silva, A. C., Kendrick-Jones, J. & Reinach, F. C. (1995). Determinants of ion specificity on EF-hands sites. Conversion of the Ca^{2+}/Mg^{2+} site of smooth muscle myosin regulatory light chain into a Ca^{2+}-specific site. *J. Biol. Chem.* **270**, 6773–6778.
49. Houdusse, A. & Cohen, C. (1996). Structure of the regulatory domain of scallop myosin at 2 Angstrom resolution—implications for regulation. *Structure*, **4**, 21–32.
50. Kuboniwa, H., Tjandra, N., Grzesiek, S., Ren, H., Klee, C. B. & Bax, A. (1995). Solution structure of calcium-free calmodulin. *Nature Struct. Biol.* **2**, 768–776.
51. Zhang, M., Tanaka, T. & Ikura, M. (1995). Calcium-induced conformational transition revealed by the solution structure of apo calmodulin. *Nature Struct. Biol.* **2**, 758–767.
52. Herzberg, O. & James, M. N. (1988). Refined crystal structure of troponin C from turkey skeletal muscle at 2.0 Å resolution. *J. Mol. Biol.* **203**, 761–779.
53. Nelson, M. R. & Chazin, W. J. (1998). An interaction-based analysis of calcium-induced conformational changes in Ca^{2+} sensor proteins. *Protein Sci.* **7**, 270–282.
54. Kawasaki, H., Nakayama, S. & Kretsinger, R. H. (1998). Classification and evolution of EF-hand proteins. *Biometals*, **11**, 277–295.
55. Shaw, G. S., Hodges, R. S. & Sykes, B. D. (1990). Calcium-induced peptide association to form an intact protein domain: ^1H NMR structural evidence. *Science*, **249**, 280–283.
56. Shaw, G. S., Hodges, R. S., Kay, C. M. & Sykes, B. D. (1994). Relative stabilities of synthetic peptide homo- and heterodimeric troponin-C domains. *Protein Sci.* **3**, 1010–1019.
57. Finn, B. E., Kordel, J., Thulin, E., Sellers, P. & Forsen, S. (1992). Dissection of calbindin D9k into two Ca^{2+}-binding subdomains by a combination of mutagenesis and chemical cleavage. *FEBS Letters*, **298**, 211–214.
58. Wojcik, J., Goral, J., Pawlowski, K. & Bierzynski, A. (1997). Isolated calcium-binding loops of EF-hand proteins can dimerize to form a native-like structure. *Biochemistry*, **36**, 680–687.
59. Thepaut, M., Strub, M. P., Cave, A., Baneres, J. L., Berchtold, M. W., Dumas, C. & Padilla, A. (2001). Structure of rat parvalbumin with deleted AB domain: implications for the evolution of EF hand calcium-binding proteins and possible physiological relevance. *Proteins: Struct. Funct. Genet.* **45**, 117–128.
60. Cox, J. A., Durussel, I., Scott, D. J. & Berchtold, M. W. (1999). Remodeling of the AB site of rat parvalbumin and oncomodulin into a canonical EF-hand. *Eur. J. Biochem.* **264**, 790–799.
61. Kretsinger, R. H. (1987). Calcium coordination and the calmodulin fold: divergent *versus* convergent evolution. *Cold Spring Harbor Symp. Quant. Biol.* **52**, 499–510.
62. Drabikowski, W., Grabarek, Z. & Barylko, B. (1977). Degradation of TN-C component of troponin by trypsin. *Biochim. Biophys. Acta*, **490**, 216–224.
63. Drabikowski, W., Kuznicki, J. & Grabarek, Z. (1977). Similarity in Ca^{2+}-induced changes between troponic-C and protein activator of 3′:5′-cyclic nucleotide phosphodiesterase and their tryptic fragments. *Biochim. Biophys. Acta*, **485**, 124–133.
64. Walsh, M., Stevens, F. C., Kuznicki, J. & Drabikowski, W. (1977). Characterization of tryptic fragments obtained from bovine brain protein modulator of cyclic nucleotide phosphodiesterase. *J. Biol. Chem.* **252**, 7440–7443.
65. Herzberg, O. & James, M. N. (1985). Structure of the calcium regulatory muscle protein troponin-C at 2.8 Å resolution. *Nature*, **313**, 653–659.
66. Sundaralingam, M., Bergstrom, R., Strasburg, G., Rao, S. T., Roychowdhury, P., Greaser, M. & Wang, B. C. (1985). Molecular structure of troponin C from chicken skeletal muscle at 3-angstrom resolution. *Science*, **227**, 945–948.
67. Babu, Y. S., Sack, J. S., Greenhough, T. J., Bugg, C. E., Means, A. R. & Cook, W. J. (1985). Three-dimensional structure of calmodulin. *Nature*, **315**, 37–40.

68. Zot, A. S. & Potter, J. D. (1987). Structural aspects of troponin–tropomyosin regulation of skeletal muscle contraction. *Annu. Rev. Biophys. Biophys. Chem.* **16**, 535–559.
69. Grabarek, Z., Tao, T. & Gergely, J. (1992). Molecular mechanism of troponin-C function. *J. Muscle Res. Cell Motil.* **13**, 383–393.
70. Takeda, S., Yamashita, A., Maeda, K. & Maeda, Y. (2003). Structure of the core domain of human cardiac troponin in the Ca^{2+}-saturated form. *Nature*, **424**, 35–41.
71. Vinogradova, M. V., Stone, D. B., Malanina, G. G., Karatzaferi, C., Cooke, R., Mendelson, R. A. & Fletterick, R. J. (2005). Ca^{2+}-regulated structural changes in troponin. *Proc. Natl Acad. Sci. USA*, **102**, 5038–5043.
72. Meador, W. E., Means, A. R. & Quiocho, F. A. (1992). Target enzyme recognition by calmodulin: 2.4 Å structure of a calmodulin–peptide complex. *Science*, **257**, 1251–1255.
73. Ikura, M., Clore, G. M., Gronenborn, A. M., Zhu, G., Klee, C. B. & Bax, A. (1992). Solution structure of a calmodulin–target peptide complex by multidimensional NMR. *Science*, **256**, 632–638.
74. Clore, G. M., Bax, A., Ikura, M. & Gronenborn, A. M. (1993). Structure of calmodulin target peptide complexes. *Curr. Opin. Struct. Biol.* **3**, 838–845.
75. Drum, C. L., Yan, S. Z., Bard, J., Shen, Y. Q., Lu, D., Soelaiman, S. *et al*. (2002). Structural basis for the activation of anthrax adenylyl cyclase exotoxin by calmodulin. *Nature*, **415**, 396–402.
76. Terrak, M., Rebowski, G., Lu, R. C., Grabarek, Z. & Dominguez, R. (2005). Structure of the light chain-binding domain of myosin V. *Proc. Natl Acad. Sci. USA*, **102**, 12718–12723.
77. Rety, S., Osterloh, D., Arie, J. P., Tabaries, S., Seeman, J., Russo-Marie, F. *et al*. (2000). Structural basis of the Ca^{2+}-dependent association between S100C (S100A11) and its target, the N-terminal part of annexin I. *Structure*, **8**, 175–184.
78. Sopkova-de Oliveira Santos, J., Oling, F. K., Rety, S., Brisson, A., Smith, J. C. & Lewit-Bentley, A. (2000). S100 protein–annexin interactions: a model of the (Anx2-p11)(2) heterotetramer complex. *Biochim. Biophys. Acta*, **1498**, 181–191.
79. Otterbein, L. R., Kordowska, J., Witte-Hoffmann, C., Wang, C. L. & Dominguez, R. (2002). Crystal structures of S100A6 in the Ca^{2+}-free and Ca^{2+}-bound states. The calcium sensor mechanism of S100 proteins revealed at atomic resolution. *Structure (Camb)*, **10**, 557–567.
80. Donato, R. (1999). Functional roles of S100 proteins, calcium-binding proteins of the EF-hand type. *Biochim. Biophys. Acta*, **1450**, 191–231.
81. Maler, L., Sastry, M. & Chazin, W. J. (2002). A structural basis for S100 protein specificity derived from comparative analysis of apo and Ca^{2+}-calcyclin. *J. Mol. Biol.* **317**, 279–290.
82. Cook, W. J., Ealick, S. E., Babu, Y. S., Cox, J. A. & Vijay-Kumar, S. (1991). Three-dimensional structure of a sarcoplasmic calcium-binding protein from Nereis diversicolor. *J. Biol. Chem.* **266**, 652–656.
83. Vijay-Kumar, S. & Cook, W. J. (1992). Structure of a sarcoplasmic calcium-binding protein from Nereis diversicolor refined at 2.0 Å resolution. *J. Mol. Biol.* **224**, 413–426.
84. Flaherty, K. M., Zozulya, S., Stryer, L. & Mckay, D. B. (1993). Three-dimensional structure of recoverin, a calcium sensor in vision. *Cell*, **75**, 709–716.
85. Tanaka, T., Ames, J. B., Harvey, T. S., Stryer, L. & Ikura, M. (1995). Sequestration of the membrane-targeting myristoyl group of recoverin in the calcium-free state. *Nature*, **376**, 444–447.
86. Ames, J. B., Ishima, R., Tanaka, T., Gordon, J. I., Stryer, L. & Ikura, M. (1997). Molecular mechanics of calcium-myristoyl switches. *Nature*, **389**, 198–202.
87. Ames, J. B., Hendricks, K. B., Strahl, T., Huttner, I. G., Hamasaki, N. & Thorner, J. (2000). Structure and calcium-binding properties of Frq1, a novel calcium sensor in the yeast *Saccharomyces cerevisiae*. *Biochemistry*, **39**, 12149–12161.
88. Bourne, Y., Dannenberg, J., Pollmann, V., Marchot, P. & Pongs, O. (2001). Immunocytochemical localization and crystal structure of human frequenin (neuronal calcium sensor 1). *J. Biol. Chem.* **276**, 11949–11955.
89. Griffith, J. P., Kim, J. L., Kim, E. E., Sintchak, M. D., Thomson, J. A., Fitzgibbon, M. J. *et al*. (1995). X-ray structure of calcineurin inhibited by the immunophilin-immunosuppressant FKBP12-FK506 complex. *Cell*, **82**, 507–522.
90. Herzberg, O., Moult, J. & James, M. N. (1986). A model for the Ca^{2+}-induced conformational transition of troponin C. A trigger for muscle contraction. *J. Biol. Chem.* **261**, 2638–2644.
91. Grabarek, Z., Tan, R. Y., Wang, J., Tao, T. & Gergely, J. (1990). Inhibition of mutant troponin C activity by an intra-domain disulphide bond. *Nature*, **345**, 132–135.
92. Fujimori, K., Sorenson, M., Herzberg, O., Moult, J. & Reinach, F. C. (1990). Probing the calcium-induced conformational transition of troponin C with site-directed mutants [see comments]. *Nature*, **345**, 182–184.
93. Wang, Z., Gergely, J. & Tao, T. (1992). Characterization of the Ca^{2+}-triggered conformational transition in troponin C. *Proc. Natl Acad. Sci. USA*, **89**, 11814–11817.
94. Gagne, S. M., Tsuda, S., Li, M. X., Smillie, L. B. & Sykes, B. D. (1995). Structures of the troponin C regulatory domains in the apo and calcium-saturated states. *Nature Struct. Biol.* **2**, 784–789.
95. Slupsky, C. M. & Sykes, B. D. (1995). NMR solution structure of calcium-saturated skeletal muscle troponin C. *Biochemistry*, **34**, 15953–15964.
96. Houdusse, A., Love, M. L., Dominguez, R., Grabarek, Z. & Cohen, C. (1997). Structures of four Ca^{2+}-bound troponin C at 2.0 Å resolution: further insights into the Ca^{2+}-switch in the calmodulin superfamily. *Structure*, **5**, 1695–1711.
97. Strynadka, N. C., Cherney, M., Sielecki, A. R., Li, M. X., Smillie, L. B. & James, M. N. (1997). Structural details of a calcium-induced molecular switch: X-ray crystallographic analysis of the calcium-saturated N-terminal domain of troponin C at 1.75 Å resolution. *J. Mol. Biol.* **273**, 238–255.
98. Finn, B. E., Drakenberg, T. & Forsen, S. (1993). The structure of apo-calmodulin. A ^1H NMR examination of the carboxy-terminal domain. *FEBS Letters*, **336**, 368–374.
99. Finn, B. E., Evanas, J., Drakenberg, T., Waltho, J. P., Thulin, E. & Forsen, S. (1995). Calcium-induced structural changes and domain autonomy in calmodulin. *Nature Struct. Biol.* **2**, 777–783.
100. Tan, R. Y., Mabuchi, Y. & Grabarek, Z. (1996). Blocking the Ca^{2+}-induced conformational transitions in calmodulin with disulfide bonds. *J. Biol. Chem.* **271**, 7479–7483.

101. Sastry, M., Ketchem, R. R., Crescenzi, O., Weber, C., Lubienski, M. J., Hidaka, H. & Chazin, W. J. (1998). The three-dimensional structure of Ca^{2+}-bound calcyclin: implications for Ca^{2+}-signal transduction by S100 proteins. *Structure*, **6**, 223–231.
102. Drohat, A. C., Amburgey, J. C., Abildgaard, F., Starich, M. R., Baldisseri, D. & Weber, D. J. (1996). Solution structure of rat apo-S100b(beta-beta) as determined by NMR spectroscopy. *Biochemistry*, **35**, 11577–11588.
103. Kilby, P. M., Van Eldik, L. J. & Roberts, G. C. (1996). The solution structure of the bovine S100B protein dimer in the calcium-free state. *Structure*, **4**, 1041–1052.
104. Drohat, A. C., Baldisseri, D. M., Rustandi, R. R. & Weber, D. J. (1998). Solution structure of calcium-bound rat S100B(betabeta) as determined by nuclear magnetic resonance spectroscopy. *Biochemistry*, **37**, 2729–2740.
105. Smith, S. P. & Shaw, G. S. (1998). A novel calcium-sensitive switch revealed by the structure of human S100B in the calcium-bound form. *Structure*, **6**, 211–222.
106. Smith, S. P. & Shaw, G. S. (1998). A change-in-hand mechanism for S100 signalling. *Biochem. Cell Biol.* **76**, 324–333.
107. Drohat, A. C., Tjandra, N., Baldisseri, D. M. & Weber, D. J. (1999). The use of dipolar couplings for determining the solution structure of rat apo-S100B(betabeta). *Protein Sci.* **8**, 800–809.
108. Rustandi, R. R., Baldisseri, D. M., Inman, K. G., Nizner, P., Hamilton, S. M., Landar, A. *et al*. (2002). Three-dimensional solution structure of the calcium-signaling protein apo-S100A1 as determined by NMR. *Biochemistry*, **41**, 788–796.
109. Fritz, G., Mittl, P. R., Vasak, M., Grutter, M. G. & Heizmann, C. W. (2002). The crystal structure of metal-free human EF-hand protein S100A3 at 1.7-Å resolution. *J. Biol. Chem.* **277**, 33092–33098.
110. Crick, F. H. C. (1953). The packing of alpha helices: simple coiled coils. *Acta Crystallog.* **6**, 689–697.
111. Chothia, C., Levitt, M. & Richardson, D. (1977). Structure of proteins: packing of alpha-helices and pleated sheets. *Proc. Natl Acad. Sci. USA*, **74**, 4130–4134.
112. Chothia, C., Levitt, M. & Richardson, D. (1981). Helix to helix packing in proteins. *J. Mol. Biol.* **145**, 215–250.
113. Skelton, N. J., Kordel, J., Akke, M., Forsen, S. & Chazin, W. J. (1994). Signal transduction *versus* buffering activity in Ca^{2+}-binding proteins. *Nature Struct. Biol.* **1**, 239–245.
114. Ikura, M. (1996). Calcium binding and conformational response in EF-hand proteins. *Trends Biochem. Sci.* **21**, 14–17.
115. Sia, S. K., Li, M. X., Spyracopoulos, L., Gagne, S. M., Liu, W., Putkey, J. A. & Sykes, B. D. (1997). Structure of cardiac muscle troponin C unexpectedly reveals a closed regulatory domain. *J. Biol. Chem.* **272**, 18216–18221.
116. Spyracopoulos, L., Li, M. X., Sia, S. K., Gagne, S. M., Chandra, M., Solaro, R. J. & Sykes, B. D. (1997). Calcium-induced structural transition in the regulatory domain of human cardiac troponin C. *Biochemistry*, **36**, 12138–12146.
117. Li, M. X., Spyracopoulos, L. & Sykes, B. D. (1999). Binding of cardiac troponin-I147-163 induces a structural opening in human cardiac troponin-C. *Biochemistry*, **38**, 8289–8298.
118. Li, Y., Love, M. L., Putkey, J. A. & Cohen, C. (2000). Bepridil opens the regulatory N-terminal lobe of cardiac troponin C. *Proc. Natl Acad. Sci. USA*, **97**, 5140–5145.
119. Gagne, S. M., Li, M. X. & Sykes, B. D. (1997). Mechanism of direct coupling between binding and induced structural change in regulatory calcium binding proteins. *Biochemistry*, **36**, 4386–4392.
120. McKay, R. T., Saltibus, L. F., Li, M. X. & Sykes, B. D. (2000). Energetics of the induced structural change in a Ca^{2+} regulatory protein: Ca^{2+} and troponin I peptide binding to the E41A mutant of the N-domain of skeletal troponin C. *Biochemistry*, **39**, 12731–12738.
121. Ababou, A. & Desjarlais, J. R. (2001). Solvation energetics and conformational change in EF-hand proteins. *Protein Sci.* **10**, 301–312.
122. Ababou, A., Shenvi, R. A. & Desjarlais, J. R. (2001). Long-range effects on calcium binding and conformational change in the N-domain of calmodulin. *Biochemistry*, **40**, 12719–12726.
123. Gellman, S. H. (1991). On the role of methionine residues in the sequence-independent recognition of nonpolar protein surfaces. *Biochemistry*, **30**, 6633–6636.
124. Zhang, M., Li, M., Wang, J. H. & Vogel, H. J. (1994). The effect of Met→Leu mutations on calmodulin's ability to activate cyclic nucleotide phosphodiesterase. *J. Biol. Chem.* **269**, 15546–15552.
125. Yuan, T. & Vogel, H. J. (1999). Substitution of the methionine residues of calmodulin with the unnatural amino acid analogs ethionine and norleucine: biochemical and spectroscopic studies. *Protein Sci.* **8**, 113–121.
126. Bunick, C. G., Nelson, M. R., Mangahas, S., Hunter, M. J., Sheehan, J. H., Mizoue, L. S. *et al*. (2004). Designing sequence to control protein function in an EF-hand protein. *J. Am. Chem. Soc.* **126**, 5990–5998.
127. Yap, K. L., Ames, J. B., Swindells, M. B. & Ikura, M. (1999). Diversity of conformational states and changes within the EF-hand protein superfamily. *Proteins: Struct. Funct. Genet.* **37**, 499–507.
128. Babini, E., Bertini, I., Capozzi, F., Luchinat, C., Quattrone, A. & Turano, M. (2005). Principal component analysis of the conformational freedom within the EF-hand superfamily. *J. Proteome Res.* **4**, 1961–1971.
129. Maune, J. F., Klee, C. B. & Beckingham, K. (1992). Ca^{2+} binding and conformational change in two series of point mutations to the individual Ca^{2+}-binding sites of calmodulin. *J. Biol. Chem.* **267**, 5286–5295.
130. Mukherjea, P. & Beckingham, K. (1993). Calcium binding site mutants of calmodulin adopt abnormal conformations in complexes with model target peptides. *Biochem. Mol. Biol. Int.* **29**, 555–563.
131. Gao, Z. H., Krebs, J., VanBerkum, M. F., Tang, W. J., Maune, J. F., Means, A. R. *et al*. (1993). Activation of four enzymes by two series of calmodulin mutants with point mutations in individual Ca^{2+} binding sites. *J. Biol. Chem.* **268**, 20096–20104.
132. Biekofsky, R. R., Martin, S. R., Browne, J. P., Bayley, P. M. & Feeney, J. (1998). Ca^{2+} coordination to backbone carbonyl oxygen atoms in calmodulin and other EF-hand proteins: ^{15}N chemical shifts as probes for monitoring individual-site Ca^{2+} coordination. *Biochemistry*, **37**, 7617–7629.

133. Biekofsky, R. R. & Feeney, J. (1998). Cooperative cyclic interactions involved in metal binding to pairs of sites in EF-hand proteins. *FEBS Letters*, **439**, 101–106.
134. Biekofsky, R. R., Turjanski, A. G., Estrin, D. A., Feeney, J. & Pastore, A. (2004). *Ab initio* study of NMR ^{15}N chemical shift differences induced by Ca^{2+} binding to EF-hand proteins. *Biochemistry*, **43**, 6554–6564.
135. Debreczeni, J. E., Farkas, L., Harmat, V., Hetenyi, C., Hajdu, I., Zavodszky, P. *et al*. (2005). Structural evidence for non-canonical binding of Ca^{2+} to a canonical EF-hand of a conventional myosin. *J. Biol. Chem.* **280**, 41458–41464.
136. Fallon, J. L. & Quiocho, F. A. (2003). A closed compact structure of native Ca^{2+}-calmodulin. *Structure*, **11**, 1303–1307.
137. Vigil, D., Gallagher, S. C., Trewhella, J. & Garcia, A. E. (2001). Functional dynamics of the hydrophobic cleft in the N-domain of calmodulin. *Biophys. J.* **80**, 2082–2092.
138. Evenas, J., Malmendal, A. & Akke, M. (2001). Dynamics of the transition between open and closed conformations in a calmodulin C-terminal domain mutant. *Structure*, **9**, 185–195.
139. Skelton, N. J., Kordel, J. & Chazin, W. J. (1995). Determination of the solution structure of Apo calbindin D9k by NMR spectroscopy. *J. Mol. Biol.* **249**, 441–462.
140. Andersson, M., Malmendal, A., Linse, S., Ivarsson, I., Forsen, S. & Svensson, L. A. (1997). Structural basis for the negative allostery between Ca^{2+}- and Mg^{2+}- binding in the intracellular Ca^{2+}-receptor calbindin D9k. *Protein Sci.* **6**, 1139–1147.
141. Svensson, L. A., Thulin, E. & Forsen, S. (1992). Proline *cis–trans* isomers in calbindin D9k observed by X-ray crystallography. *J. Mol. Biol.* **223**, 601–606.
142. Kordel, J., Skelton, N. J., Akke, M. & Chazin, W. J. (1993). High-resolution solution structure of calcium-loaded calbindin-d(9k). *J. Mol. Biol.* **231**, 711–734.
143. Rety, S., Sopkova, J., Renouard, M., Osterloh, D., Gerke, V., Tabaries, S. *et al*. (1999). The crystal structure of a complex of p11 with the annexin II N-terminal peptide. *Nature Struct. Biol.* **6**, 89–95.
144. Pettersen, E. F., Goddard, T. D., Huang, C. C., Couch, G. S., Greenblatt, D. M., Meng, E. C. & Ferrin, T. E. (2004). UCSF chimera—a visualization system for exploratory research and analysis. *J. Comput. Chem.* **25**, 1605–1612.
145. Schumacher, M. A., Crum, M. & Miller, M. C. (2004). Crystal structures of apocalmodulin and an apocalmodulin/SK potassium channel gating domain complex. *Structure (Camb)*, **12**, 849–860.
146. Chattopadhyaya, R., Meador, W. E., Means, A. R. & Quiocho, F. A. (1992). Calmodulin structure refined at 1.7 Å resolution. *J. Mol. Biol.* **228**, 1177–1192.
147. Rao, S. T., Wu, S., Satyshur, K. A., Ling, K. Y., Kung, C. & Sundaralingam, M. (1993). Structure of *Paramecium tetraurelia* calmodulin at 1.8 Å resolution. *Protein Sci.* **2**, 436–447.
148. Rupp, B., Marshak, D. R. & Parkin, S. (1996). Crystallization and preliminary X-ray analysis of two new crystal forms of calmodulin. *Acta Crystallog. sect. D*, **52**, 411–413.
149. Yun, C. H., Bai, J., Sun, D. Y., Cui, D. F., Chang, W. R. & Liang, D. C. (2004). Structure of potato calmodulin PCM6: the first report of the three-dimensional structure of a plant calmodulin. *Acta Crystallog. sect. D*, **60**, 1214–1219.
150. Fenn, T. D., Ringe, D. & Petsko, G. A. (2003). POVScript+: a program for model data visualization using persistence of vision ray-tracing. *J. Appl. Crystallog*. **36**, 944–947.
151. Kraulis, P. J. (1991). MOLSCRIPT: a program to produce both detailed and schematic plots of protein structures. *J. Appl. Crystallog*. **24**, 946–950.

Edited by P. Wright

(Received 26 January 2006; received in revised form 25 March 2006; accepted 30 March 2006)
Available online 21 April 2006